Lithofacies: Core to Model

Digital Lithofacies Description System

	1	2	3	4	5
CODE	Rock Type	Dunham / Folk Classification	Grain Size	Principal Pore Size	Argillaceous Content
9	Evaporite	**cobble** conglomerate	cobble (**>64mm**)	cavern vmf (**>64mm**)	Frac-fill 10-50%
8	Dolomite	**sucrosic** / pebble congl.	pebble (**4-64mm**)	med-lrg vmf (**4-64mm**)	Frac-fill 5-10%
7	Dolomite-Limestone	**bafflestone** / vcrs ss	vcrs sand (**1-4mm**)	sm vmf (**1-4mm**)	Shale **>90%**
6	Dolomite-Siliciclastic	**grainstone** / crs ss	crs sand (**500-1000um**)	crs (**500-1000um**)	Shale **75-90%**
5	Limestone	**pkst-grnst** / med ss	med sand (**250-500um**)	med (**250-500um**)	Shale **50-75%**
4	Carbonate-Siliciclastic	**packstone** / fn ss	fn sand (**125-250um**)	fn (**125-250um**)	Shale **25-50%**
3	Siliciclastic-Carbonate	**wkst-pkst** / vfn ss	vfn sand (**62-125um**)	pin-vf (**62-125um**)	Shale **10-25%**
2	Marine Siliciclastic	**wackestone** / crs silt	crs silt (**31-62um**)	pinpoint (**31-62um**)	wispy **5-10%**
1	Continental Siliciclastic	**mdst-wkst** / vf-m silt	vf-m silt (**4-31um**)	microporous (**<31um**)	trace **1-5%**
0	Shale	**mudstone** / shale / clay	clay (**<4um**)	**nonporous**	Clean **<1%**

Digital Description	Lithofacies Code	Lithofacies Class
1/>2	0	Continental SS
1/2	1	Continental Silt
1/0-1	2	Continental ShlySilt
0,2/<3	3	Marine Shale & Silt
3-8/0-1	4	Mdst/Mdst-Wkst
3-8/2-3	5	Wkst/Wkst-Pkst
6-8/8/<3	6	Vfxln Sucrosic (Dol)
3-8/4-5	7	Pkst/Pkst-Grnst
3-8/6-7	8	Grnst/PA Baff
7-8/8/>2	9	F-Mxln Sucrosic Moldic Dol
2/>2	10	Marine SS

Classifying lithofacies in a digital form facilitated changes in classification criteria and correlation of lithofacies with core and log properties while determining optimal lithofacies class boundaries. Five key variables and digital code for eleven lithofacies are shown. Example: 13323, is a continental v. fine-grained

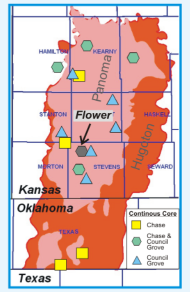

14 continuous cores selected for lithofacies analysis based on length, geography, and availability of core analysis and wireline log data.

Eleven Lithofacies Classes

Classes determined by four factors:

- Maximum number recognizable by neural networks
- Minimum needed to represent lithologic and petrophysical heterogeneity
- Maximum distinction of core petrophysical properties among classes
- Relative contribution of a class to storage and flow

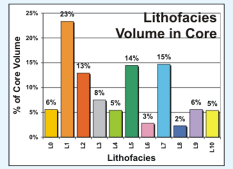

L0 Continental sandstone
Example: Coarse silt to very fine-grained sandstone, mostly quartz. Adhesive meniscate burrows (Hasiotis, 2005, personal communication). Low-relief migrating eolian system. Digits: 13322.

L1 Continental coarse siltstone
Example: Coarse quartz silt. Rhizolith (Rz) and root traces with reduction haloes (Ho). Savannah, slow accumulation by airfall, stabilized by vegetation and soil processes. Digits: 12213.

L2 Continental shaly siltstone
Example: Fine to medium-grained quartz silt and clay. Caliche (Ca), rhizolith (Rz), and root traces with reduction haloes (Ho). Coastal plain, slow accumulation by airfall, stabilized by vegetation and soil processes. Digits: 11114.

L3 Marine siltstone and shale
Example: Very fine-grained shaly siltstone. Siliciclastic dominated shelf at maximum flooding. Plug phi = 4.6%, k = 0.0001 md. Digits: 21104

L4 Mudstone and mudstone-wackestone
Example: Silty mudstone-wackestone. Mini-stylolites (Ms), burrowed in part (Bh), fusulinids (Fs). Low energy shelf near maximum flooding. Plug phi = 3.1%, k = 0.00239 md. Digits: 41113.

L5 Wackestone and wackestone-packstone
Example: Slightly dolomitized wackestone. Low energy normal marine shelf. Full-diameter phi = 15.2%, k = 0.413 md. Digits: 52111.

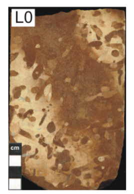

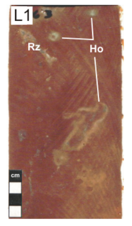

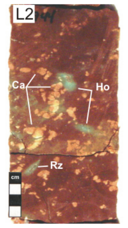

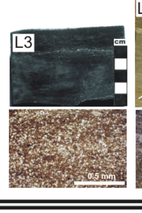

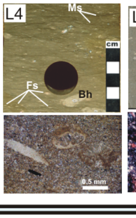

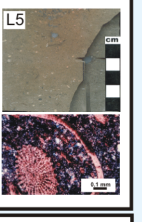

L6 Very fine crystalline sucrosic dolomite
Example: Dolomitized mudstone). An = anhydrite, Mo = molds. Restricted, protected lagoon. Plug phi = 13.9%, k = 1.37 md. Digits: 88120.

L7 Packstone and packstone-grainstone
Example: Medium- to coarse-grained bioclastic-oncoid packstone. An = anhydrite cement. Carbonate sand shoal on open shelf. Full-diameter phi = 16.4%, k = 5.98 md. Digits: 54520.

L8 Grainstone *or* phylloid algal bafflestone.
Lithofacies lumped due to small populations and similar core and wireline log properties and were lumped because of their small populations.

Example a: Medium-coarse grained oncoid-peloid grainstone Carbonate sand shoal on restricted shelf. Full-diameter phi = 18.8%, k = 39.0 md. Digits: 56540.

Example b: Phylloid algal bafflestone. Pm = Phylloid algal blade molds An = anhydrite cement. Phylloid algal mound on slightly restricted shelf. Full-diameter phi = 20.6, k = 1141 md. Digits: 57770.

L9 Fine to medium crystalline moldic dolomite
Example: Dolomitized medium-coarse grained grainstone. Mo = molds, An = anhydrite cement. Carbonate sand shoal on an open shelf. Full-diameter phi = 22.3%, k = 275 md. Digits: 88550

L10 Marine sandstone
Example: Very coarse silt to very fine-grained sandstone, well sorted, sub arkose. Planar (Px) and ripple (Rx) cross bedding and vertical burrows (Bv), patchy anhydrite cement (An). Tidal flat. Full-diameter phi = 20.8%, k = 48.2 md. Digits: 23321.

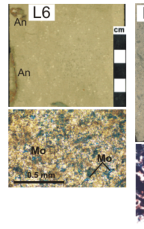

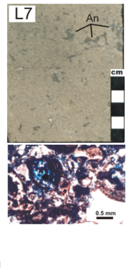

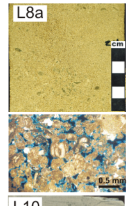

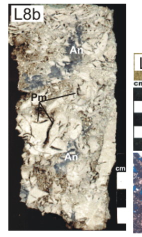

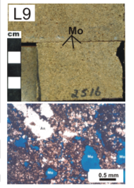

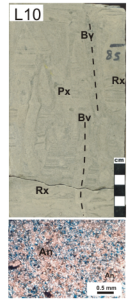

Depositional Models

Sedimentary Cycles

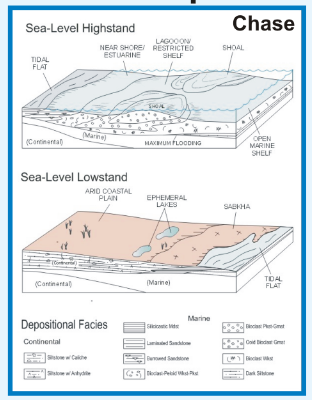

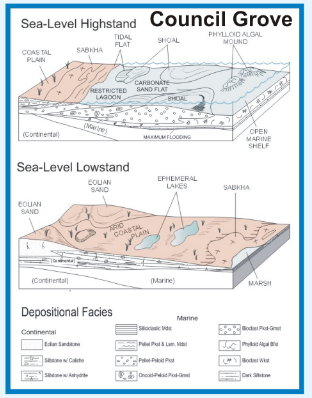

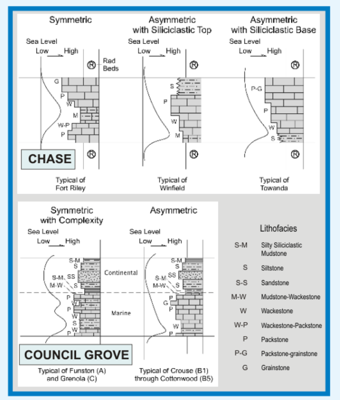

Depositional models:

Illustrated are environments and distribution of associated lithofacies on the Hugoton shelf for “typical” Chase and Council Grove cycles during the falling sea level stage of the marine highstand and at maximum sea-level lowstand. Subtle differences may be related to a change in climatic conditions from more icehouse to more greenhouse conditions in the Permian.

Sedimentary cycles:

Chase cycles are from Olson et al., 1997. We extend the cycle and sea level curve through continental half-cycles in the Council Grove based on earlier work (Dubois and Goldstein, 2005). **Five “cycle types”** are distinguished on the basis of lithofacies stacking pattern and inferred relative sea level curve. Vertical succession of lithofacies in a shoaling upward pattern is a result of depositional environments changing across the shelf in response to rapid sea level fluctuation. Council Grove cycles are typically more asymmetric than the Chase cycles and tend to have better developed, thin, packstone-grainstone lithofacies at the base of the marine half-cycle. **Vertical histograms of predicted lithofacies** in model node wells also demonstrate the asymetry.

Vertical Histograms Predicted Lithofacies

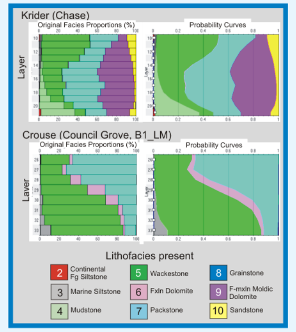

Predict Lithofacies with Neural Networks Trained on Core

1. **Generate training set (lithofacies tied to e-log and two geologic variables)**
2. **Optimize neural network parameters**
3. **Train and test neural networks**
4. **Predict lithofacies in 1350 wells using an automated process**

- Marine-nonmarine (MnM) and relative position to base (RelPos) are calculated from the tops set and add geologic information
- Misallocation is based on a cost matrix and is proportional to the “distance” in lithofacies code units in the predicted lithofacies from actual (L7 vs. L3 carries higher cost than L7 vs. L8).
- Six neural network models, one with PE and one without, for Upper Chase, Lower Chase and Council Grove

Neural Network Structure

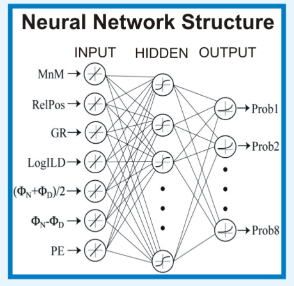

Optimal Parameters

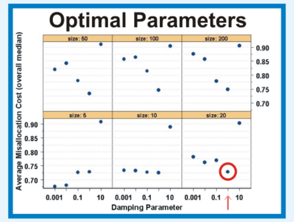

Cross-validation determines optimal neural network hidden-layer nodes (20) and damping parameter (1). Misallocation cost is metric.

“Jacknife” test Chase (NoPE)

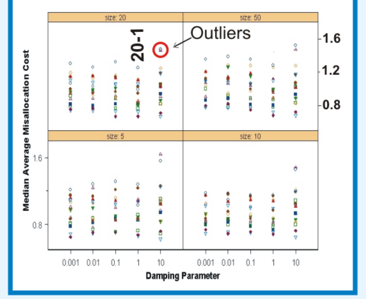

Jacknife approach (predict lithofacies for well withheld from training) demonstrates effective training. Most wells have low misallocation costs (0.6-1.1) for optimal parameters (20-1). A few wells have problems with other parameters.

Probability: Predicted - Actual (for a cored well)

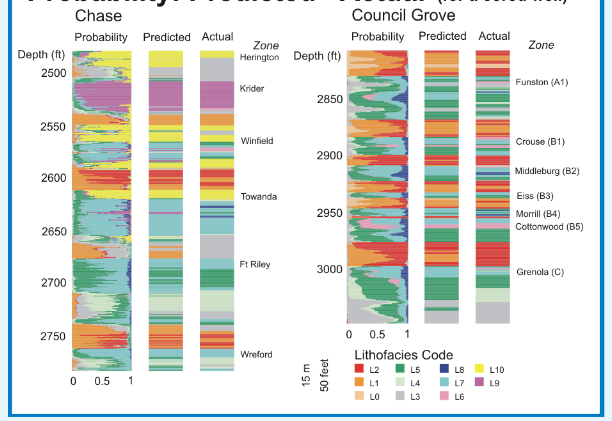

Core Petrophysics

Porosity

Histogram of routine helium porosity for Chase and Council Grove nonmarine continental (NM) sandstones and siltstones (A) and limestones (B). Porosity generally increases with increasing grain size in siliciclastics and with decreasing mud content from mudstone through grainstone (Baff-bafflestone, Grst-grainstone, Pkst-packstone, Wkst-wackestone, Mdst-mudstone).

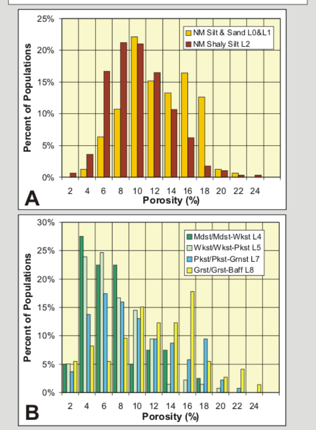

Lithofacies Code	*In situ* Klinkenberg Permeability logkik= AlogPhii+B A	*In situ* Klinkenberg Permeability logkik= AlogPhii+B B
0	7.90	-9.00
1	7.90	-9.43
2	7.90	-9.80
3	8.31	-10.70
4	7.98	-9.68
5	6.26	-7.53
6	7.10	-8.71
7	6.17	-6.82
8	8.24	-8.44
9	6.30	-6.59
10	8.31	-9.70

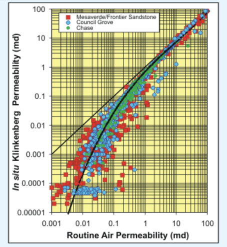

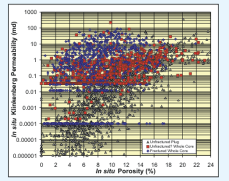

Permeability

Fundamental to construction of the reservoir geomodel is the population of cells with the basic lithofacies and their associated petrophysical properties- porosity, permeability, and fluid saturation. Petrophysical properties vary among the eleven major lithofacies. Accurate permeability prediction requires input of lithofacies, use of properties that represent reservoir conditions, and filtering of full-diameter data to avoid microfractured core.

Core-measured *in situ* Klinkenberg permeabilities (k_{ik}) range from 0.00002-400 md ($2*10^{-8}$0.4 μm^2). Over approximately 75% of all rocks in the Hugoton exhibit an *in situ* Klinkenberg permeability less than 1 md (0.001 μm^2). Both continental and carbonate rocks exhibit a significant decrease in permeability below approximately 1 md (0.001 μm^2) due to the influence of Klinkenberg gas slippage and confining stress combined (Figure). Whole core (full-diameter) values diverge from matrix (plug) values at porosities less than ~10% and matrix permeability of ~0.5 md reflecting the influence of microfracture(s) on permeability in whole core samples with porosity < 10%. Above 10 % porosity influence of microfractures(s) is small (Figure).

Permeability is a function of several variables including primarily pore throat size, porosity, grain size and packing (which controls pore body size and distribution), and bedding architecture. Lithofacies-specific equations were developed to predict permeability using porosity as the independent variable. As with many sedimentary rocks, the relationship between permeability and porosity can be approximated by a power-law functions where equation parameters are shown in the accompanying table (Figures):

$$k_{ik} = A\,\phi_i^{\,B}$$

Trend lines exhibit a standard error of prediction ranging from 3.3X to 9X depending on the lithofacies.

The good correlation over eight orders of magnitude of Principal Pore Throat Diameter (PPTD) shows the predominant influence that pore-throat size exerts on permeability and explains permeability changes with grain size and Dunham classification at a given porosity. Second Y-axis shows corresponding threshold entry heights necessary for gas column to enter sample for gas pressure and temperature conditions in Hugoton area. The correlation between k_{ik} and PPTD can be expressed:

$$PPTD = 2.2\,k_{ik}^{0.42}$$

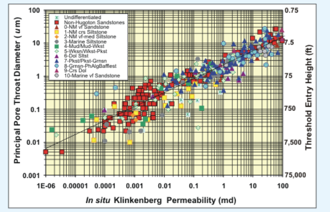

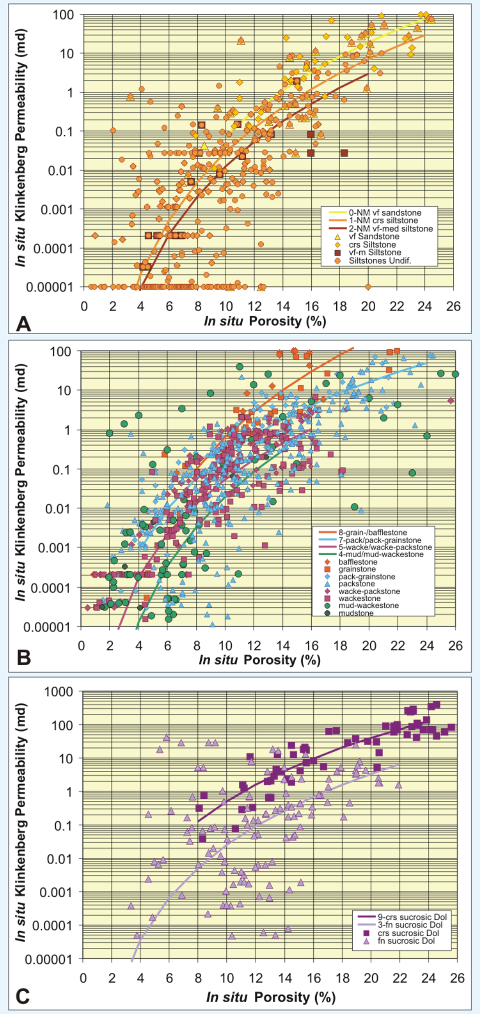

Water Saturation and Capillary Pressure

Capillary pressures and corresponding water saturations (*Sw*) vary among lithofacies, and with porosity/permeability and gas column height. Threshold entry pressures and corresponding heights above free water level are well correlated with permeability (Figure) consistent with the relationship between pore throat size and permeability.

Synthetic capillary pressure curves were constructed based on capillary pressure-porosity-permeability-lithofacies relationships. Curves are defined by two terms that vary with lithofacies and porosity. Modeled capillary pressure curves for two important lithofacies (Figure) illustrate that with decreasing porosity (and associated permeability) threshold entry heights and transition zone heights increase. Example capillary pressure curves for different lithofacies at a given 10% porosity (Figure) illustrate the significant differences in *Sw* that can exist among lithofacies at any given height above free water level. Because differences decrease with increasing height, saturations for all lithofacies approximately approach a similar “irreducible” saturation at gas column heights above ~300 ft (90 m) except for low porosity rocks where saturation differences are still evident.

Utilizing the capillary pressure model, it was possible to predict water saturation for any given lithofacies and porosity at any given height above free water saturation and thus populate every gridcell in the 3D geomodel with water saturation values.

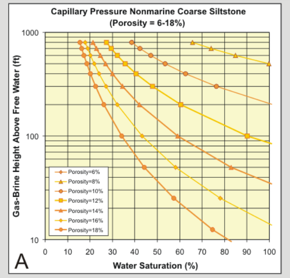

LithCode	Pc Slope "Pchs" Pchs= APhii+B A1	Pc Slope "Pchs" Pchs= APhii+B B1	Pc Threshold Height logPche= APhii+B (ft) A2	Pc Threshold Height logPche= APhii+B (ft) B2
0	0.1980	-5.3190	-0.1940	4.0500
1	-0.1530	0.0990	-0.1940	4.2500
2	-0.1530	0.0990	-0.1940	4.4300
3	-0.1530	0.0990	-0.2060	4.3460
4	-0.0660	-1.1500	-0.1220	3.3000
5	-0.0420	-1.0000	-0.1190	3.0600
6	0.0041	-1.2190	-0.0540	2.6300
7	-0.0063	-1.6570	-0.0550	1.9700
8	0.0000	-1.6300	-0.0310	1.5200
9	0.1280	-3.8980	-0.0540	1.7000
10	0.1980	-5.1390	-0.0795	2.5170

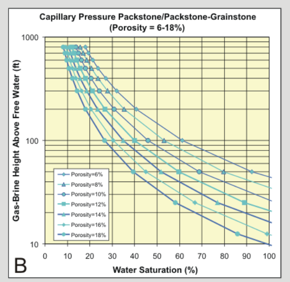

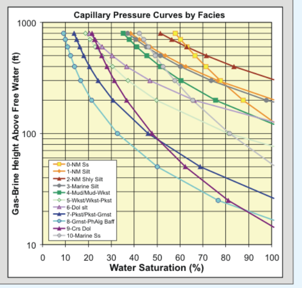

Relative Permeability

Gas and water drainage relative permeability curves reveal several characteristics similar to other low-permeability rocks. Water permeability, even at 100% Sw, is less than Klinkenberg gas permeability and decreases with decreasing permeability. Gas relative permeability is less than the absolute gas permeability at all water saturations greater than zero and gas relative permeability decreases significantly as *Sw* increases above 50%. Relative permeabilities can be reasonably modeled using Corey-type equations (Figure), similar to other low-permeability rocks (Byrnes, 2003).

Relative gas permeability (A) and water relative permeability (B) curves for 32 samples of various lithofacies. Black curves represent predicted values for the Corey-type equation model:

$$k_{rg} = (1\ \ (S_w-S_{wc,g})/(1-S_{gc}-S_{wc,g}))^p\ (1-((S_w-S_{wc,g})/(1-S_{wc,g}))^2)$$

$$k_{rw} = ((S_w-S_{wc})/(1-S_{wc}))^q\ (k_w/k_{ik})$$

where S_{wc} is the critical water saturation, $S_{wc,g}$ is the critical water saturation for gas flow, and all saturation terms are in fractions. Black curves represent mean values of exponents p = 1.3 for gas curve and q = 8.3 for water curve while grey bounding curves represent outer limits of curves using exponents p = 1.3±0.4 and q = 8.3±3 which represent the range exhibited by the sample set, which had 0.1 md $< k_{ik} <$ 50 md.

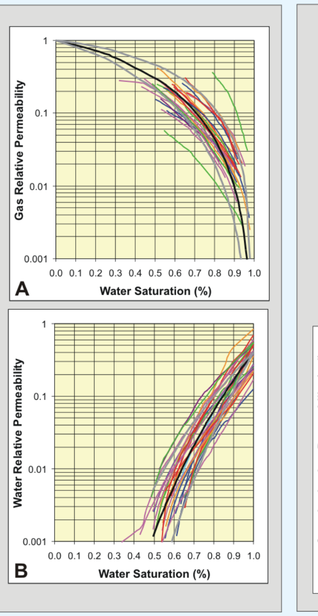

Matrix vs Fracture and Scale

Close correspondence of DST permeabilities and upscaled plug-scale permeabilities is interpreted to indicate that production from many wells is controlled by matrix permeability and not fractures.Good correlation down to ~0.5 md shows matrix-scale control of flow in the region of DST investigation. Below 0.5 md, microfractures in full-diameter core result in permeabilities higher than in the unfractured reservoir. Higher DST than core plug permeabilities can be interpreted to indicate that formation is not fractured in the range of investigation and that plug sampling density was probably not adequate to properly sample lower range of permeability.

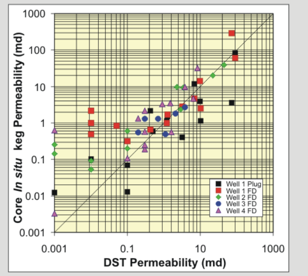

Correct Log Porosity

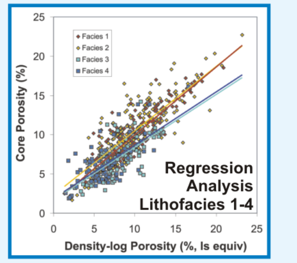

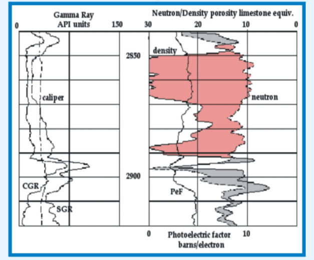

Severe Gas Effect in Krider (Chase)

Accurate porosity derived from wireline logs is critical to estimating reservoir volumes and gas in place.

Corrections for **environmental effects (washouts)** were accomplished by establishing a lithofacies-dependent porosity cutoff, above which the mean core porosity for that lithofacies is assigned. Corrections for **gas effect and mineralogy** are based on equations derived through regression analysis relating core porosity to Neutron and Density log porosity measurements. Corrections were applied by an **automated process** for the 1350 node wells.

Equations

Corrected Porosity = A + B*Dphi + C*Nphi

	LithCode	Porosity Correction Intercept A	Porosity Correction Dphi Coefficient B	Porosity Correction Nphi Coefficient C	Washout Correction PhiND Threshold Thresh	Washout Correction PhiCorr Replace Value RepVal
Cont. SS	L0	0.0178	0.8434	0.0000	0.2000	0.0700
Cont. Crs Silt	L1	0.0178	0.8434	0.0000	0.2000	0.0700
Cont. Fn Silt	L2	0.0178	0.8434	0.0000	0.2000	0.0700
Mar. Silt	L3	0.0185	0.6619	0.0000	0.2000	0.0700
Mudstone	L4	0.0185	0.6619	0.0000	0.2000	0.0700
Wackestone	L5	0.0000	0.6102	0.3985	0.2250	0.1000
Fxln Dolomite	L6	4.6303	0.5321	0.2591	0.2250	0.1000
Packstone	L7	0.0000	0.6102	0.3985	0.2250	0.1000
Grainstone	L8	0.0000	0.6102	0.3985	0.2250	0.1000
Mxln Moldic Dol.	L9	4.6303	0.5321	0.2591	0.2250	0.1000
Mar. SS	L10	5.2480	0.4730	0.1510	0.2250	0.1000

Before Corrections

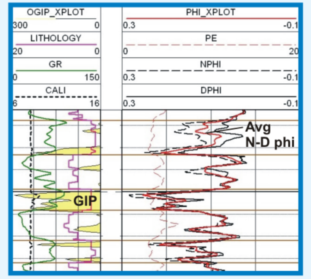

After Corrections

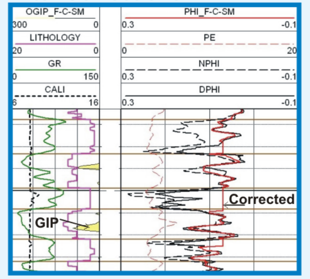

Estimate Free Water Level

Estimating the free water level (FWL) position is critical for calculating water saturations using capillary pressures and the height above FWL. Hugoton field has a sloped gas-water contact, and we interpret a sloped FWL that is several 100's of feet (100's m) higher at the west updip margin than on the east downdip limits (Garlough and Taylor, 1941; Hubbert, 1953, 1967; Pippin, 1970; Sorenson, 2005).

We define the gas-water contact as the lowest position in the reservoir that a well can produce gas economically (low water volume), and the free water level as the datum where gas-brine capillary pressure is zero. Initial reservoir desaturation may not occur for some lithofacies until several tens or hundreds of feet (10s-100s m) above the free water level (threshold entry height). For typical reservoir rocks in the study area, packstone-grainstone 8-10% porosity, the FWL ranges from 50-70 ft (9-21 m) below the “gas-water” contact, a point at which the water saturation is approximately 70%.

FWL is estimated on the basis of four indicators: (1) base of lowest perforations; (2) formation fluid resistivity estimated from wireline logs; (3) calculation of the FWL for an estimated original gas in place (OGIP), and 4) pressure measurements of deep water productive intervals.

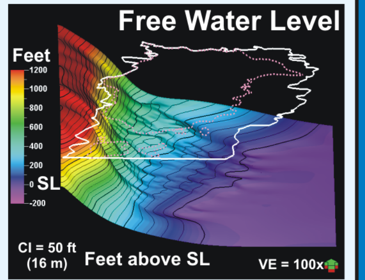

Chase and Council Grove have common FWL that is sloped.

Height Above FWL